Journal of Harbin Engineering University
ISSN: 1006-7043

Vol 44 No. 7
July 2023

Determination of Responses of Seismic-Resistant Building Structures with Various Triple Friction Pendulum Configurations

Vivi Dwi Darmawati[1] and Tavio[1]*

[1]Department of Civil Engineering, Institut Teknologi Sepuluh Nopember, Surabaya, Indonesia.
*Corresponding author

Abstract

An earthquake is a disaster that causes vibrations and can cause damage to infrastructure. Therefore, there is an urgent need to provide buildings that are safe against severe earthquakes to avoid structural failure. One of the most effective systems for buildings against earthquakes is the seismic isolation system. This study aims to analyze and evaluate the efficiency of the configuration of the isolation system on the response of building structures to earthquakes. The method used is to apply it without isolators, isolators on the 4th floor, isolators on the 1st and 4th floors between 2 different buildings, namely A and B. From the results of the analysis of the most rigid building, namely building A when viewed from the building period. the biggest earthquake that occurred was in the imperial valley based on the results of displacement, inter-story drift, and story shear.

Keywords: Building structures, Disaster risk reduction, Isolation system, Structural response, Triple friction pendulum.

1. Introduction

Indonesia is located on top of a stack of three large plates, i.e., the Eurasian (Europe-Asia) plate from the North, the Indo-Australia plate from the South, and the Pacific place from the east, causing the country to be susceptible to earthquakes [1,2]. The severe impacts of earthquakes, among others, are casualties of human life, loss of properties, infrastructure damage, or even collapse. The cause of the loss of life and economy is solely due to the collapse of buildings built by humans during an earthquake [3,4]. There are several ways to protect buildings against earthquakes, such as by making the building structurally ductile (e.g., using ductile materials) [5] with a higher level of damage, or in other words, by ensuring that the performance of the building is higher. This can be done by reducing the impact of earthquake damage and achieving better comfort during an earthquake by introducing an isolation system to the building [6].

Seismic isolation provides low horizontal rigidity of a building by shifting the fundamental period of the structure out of the high earthquake range and separating the superstructure from ground motion [7,8].

The dynamic response of the structure can be reduced by the installation of an isolation structure device [9,10]. The use of base isolations in houses and buildings has been widely proven to provide better performance in reducing damage during earthquakes [11]. The use of base isolations is very easy for new buildings but kind of complicated and has relatively higher costs for retrofitting applications, requiring excavation and load transfer, while the concept and application of inter-story isolation were studied both experimentally and analytically and were relatively simple, inexpensive, and hassle-free [12]. One of the basic isolation technologies is the friction pendulum system (FPS).

Friction Pendulum System (FPS) is one type of basic isolation technology, and its effectiveness for isolating transmitted seismic energy has been validated by comprehensive experimental and numerical studies [13,14]. FPS works using curved sliding surfaces that cause the structure to move back to its original position based on the principle of pendulum motion [15]. Part of the FPS applied in this study is the Triple Friction Pendulum System (TFPS), which is a pendulum developed by Fenz and Constantinou by modifying the DCFP system [16,17]. This modification improves the

relative performance and measurement capacity of TCFP energy isolations compared to DCFP. The surfaces of each joint piece are convex and concave so that they can easily slide over each other, providing seismic isolation and energy dissipation. The system has four sliding surfaces where the desired seismic capability can be achieved for isolation by adjusting each surface's radius of curvature and coefficient of friction [15]. One of the studies on the ability of buildings to withstand earthquake loads with the theme curve develops school buildings with and without retrofit due to earthquake and tsunami loads found that the percentage probability of structural damage decreased after the structure was retrofitted and the results of its analysis showed that strengthening the building structure using concrete casing reduces the possibility of damage to the building structure due to earthquake loads of 42.06% in the level of extensive damage and 4.42% in the level of total damage in the PGA. 0.6g, while reducing the possibility of damage to buildings due to tsunami loads by 45.53% at the extensive damage level and by 26.32% at the total damage level at a tsunami inundation depth of 4.5m [22].

2. Isolators' placement in two different buildings

The research was conducted in two different types of buildings, namely Buildings A and B with the placement of insulators between the same buildings, namely on floors 1 and 4. This aims to determine the most effective isolation placement in terms of structural response or performance due to earthquake hazards. The case study is used for a low-rise building, namely 8 floors. The buildings were designed with the same floor number, different layouts, and the same 8-story height. The placement and selection of the location of the insulation applied to the floor is then used as an issue to evaluate the floor displacements and the floor shear between buildings. Building code and seismic according to Indonesian standards. The results of this study provide new information about the optimal response or performance related to the placement or selection of insulation locations between floors and then assist in the design of isolated buildings in the future.

3. Results

3.1 General Description of Building Structure

Workability is one of the significant limitations of FRC for better performance of hardened concrete (Liew and Akbar, 2020). The kind and volume of RSF significantly impact the workability of concrete, which is the main criterion.

3.2 Seismic Force Application

The seismic force-resisting system needs to consider the response modification coefficient, deflection amplification coefficient, system overstrength factor, and structural total height limitation. The designed seismic force for the seismic force-resisting system should meet one of the structural types specified in Table 12 of SNI 1726:2019 [19]. According to Article 7.2 of SNI 1726:2019 [19], the seismic force-resisting system is determined by parameters, such as response modification coefficient (***R***), deflection amplification coefficient ($\boldsymbol{C_d}$), system overstrength factor ($\boldsymbol{\Omega_o}$), and structural total height limitation.

3.2.1 Stiffness and natural period of the structure

The structural design needs to consider the natural rigidity and period of the structure. Stiffness can be defined as the force required to deform one unit. The rigidity of a structure is inversely proportional to its natural period, as evidenced by its formulation as follows:

$$T = \frac{1}{f} = \frac{2\pi}{\omega} \quad (1)$$

$$\omega = \sqrt{\frac{k}{m}} \quad (2)$$

The relationship between stiffness (k) and the natural period of the structure (T) is inversely related.

$$T \cong \frac{1}{\sqrt{k}} \quad (3)$$

The relationship between stiffness (k) and the natural period of the structure (T) is inversely related.

$$T_{minimum} = T_a = C_t h_n^x \quad (4)$$

$$T_{maksimum} = C_u T_a \quad (5)$$

Thus, it can be concluded that the greater the natural period of a structure, the less stiffness the structure has. This becomes the basis for estimating the period and stiffness according to the structural design.

3.2.2 Seismic Response Coefficient

According to SNI 1726:2019 [19] Article 7.8.1.1, the seismic response coefficient is determined by the following formula:

$$C_{s-natural} = \frac{S_{D1}}{T\left(\frac{R}{I_e}\right)} \quad (6)$$

C_s value should not exceed the following equation:

$$C_{s-max} = \frac{S_{DS}}{\left(\frac{R}{I_e}\right)} \quad (7)$$

C_s value should not be less than:

$$C_{s-min} = 0.044 S_{DS} I_e \geq 0.01 \quad (8)$$

For structures located in areas where S_1 is equal to or greater than 0.6g, C_S cannot be less than:

$$\boldsymbol{C_{s-min}} = \frac{\boldsymbol{0.5 S_1}}{\left(\frac{\boldsymbol{R}}{\boldsymbol{I_e}}\right)} \quad (9)$$

3.2.3 Design Response Spectrum

The spectral response is the maximum response of an SDOF (Single Degree of Freedom) structural system in the form of acceleration, velocity, or displacement of a structure due to loading with a certain pattern. The spectral response curve can show the maximum relative displacement (S_d), maximum relative velocity (S_v), and maximum total acceleration (S_a) on the y-axis and the natural period of the structure on the x-axis.

3.2.4 Load Combinations

The load combinations applied to the structure must be designed in such a way that the design strength of the structure exceeds the influence of the factored load. Based on SNI 1726:2019 Article 4.2.2 [19], the factored load combinations include: (1) 1.4D; (2) 1.2D + 1.6L + 0.5L_r; (3) 1.2D + 1.6L_r + 1.0L; (4) 1.2D + 1.0L + 0.5L_r; (5) 0.9D; (6) 1.2D + 1.0E_v + 1.0E_h + 1.0L; (7) 0.9D – 1.0E_v + 1.0E_h. D is the dead load including self-weight, L is the live load, L_r is the live load of the roof, and E is the earthquake load.

3.2.5 Inter-story Displacement

The inter-story displacement is defined as the difference in the center of mass above and below the level under consideration. Determination of the designed displacement, Δ_α shall not exceed the allowable story displacement. Inter-story is defined in SNI 1726:2019 Article 7.8.6 [19] as:

$$\delta_x = \frac{C_d \delta_{xe}}{I_e} \quad (10)$$

3.2.6 Isolator System

The isolation system used in the study is a triple friction pendulum (TFP) bearing. The cross-sectional elevation and dimensional properties of the TFP are illustrated in Fig. 1.

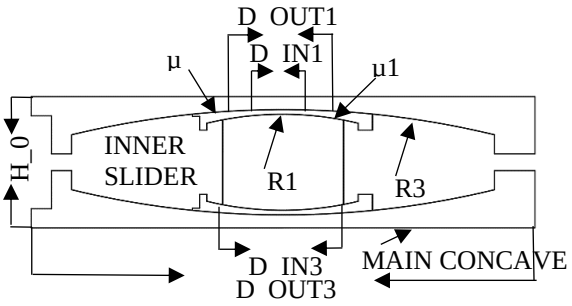

Figure 1: Cross-sectional elevation view and dimensional properties of triple friction pendulum (TFP) bearing isolation system [18]

The properties and parameters of triple friction pendulum bearing are given in Table 1

Table 1: Properties and parameters of triple friction pendulum bearings

Surface	R (m)	H (m)	μ	D_{out} (m)	D_{in} (m)
1	5	2	5	0.4	0.1
3	6	1	6	1	0.5

3.3 Additional Building Isolation

3.3.1 Addition of Isolations to Building Structure A

TFP was used in both buildings using the same TFP with a difference in the number of bearings. Building Structure A placed the isolations on the 1st, 5th, and 7th stories with a total of 20 bearings on each story (Fig. 2).

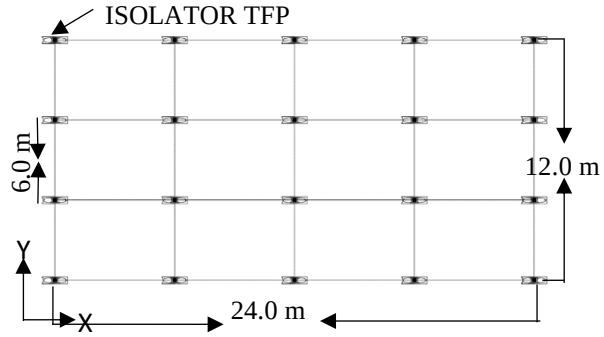

Figure 2: Isolations on the 1st story

3.3.2 Addition of Isolations to Building Structure B

Building Structure B placed the isolations on the 1st story with a total of 20 bearings. The 5th and 7th stories used 12 bearings for each story (Figs. 3).

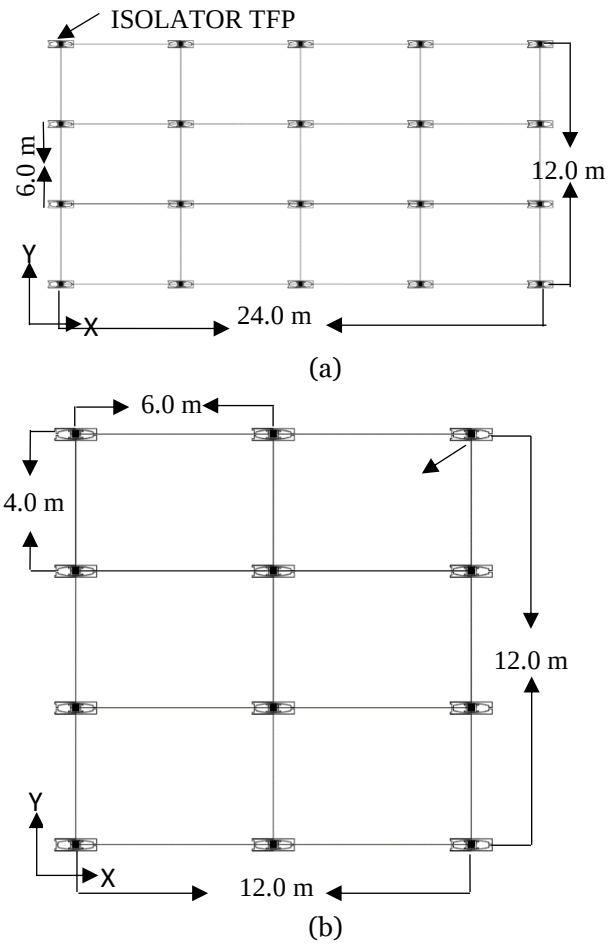

Figure 3: Isolations on the 1st (a) and Isolations on the 5th story (b)

3.4 Structure Modeling

Structural modeling was carried out by using the structural analysis program. Both Building Structures A and B were assigned using identical member sizes and dimensions (Table 2).

Table 2: Dimensional structure data

Floor	Beam Dimensions (mm)	Column Dimensions (mm)	Slab Thickness (mm)
Floors 1-7	B1 350x350 B2 450x450	K 650x850	S120
Floor 8	B1 350x350 B2 450x450	K 650x850	S 100

3.4.1 Earthquake Loading Conforming SNI 1726:2019

The calculation of the earthquake load or story shear force of the building structure used the linear time-history dynamic analysis method with a surface peak ground acceleration (PGA) of 0.3152*g*. Referring to the building function category in SNI 1726:2019 [19], it can be defined as Category IV such that according to the spectral response parameters of SNI 1726:2019, the importance factor *I* equals 1 and the response modification coefficient (*R*) for special moment reinforced concrete frames is determined in Table 12 of SNI 1726:2019 and equals 8.

The dynamic earthquake data used in the study was obtained from the website peer.berkeley.edu. The designed earthquake load for the building used time-history earthquake data (ground motion) shown in Fig. 7 (plotted reference time history). By converting it into spectral response data at the location of the building, the plotted reference spectral response can be obtained, as seen in Fig. 8. It is then matched to the spectral response at the location of the building (plotted matched spectral response), as can be seen in Fig. 8. Then, it is converted back to an accelerogram as shown in Fig. 4 (a plotted matched time history). The blue and red colors indicate the plotted reference and match, respectively.

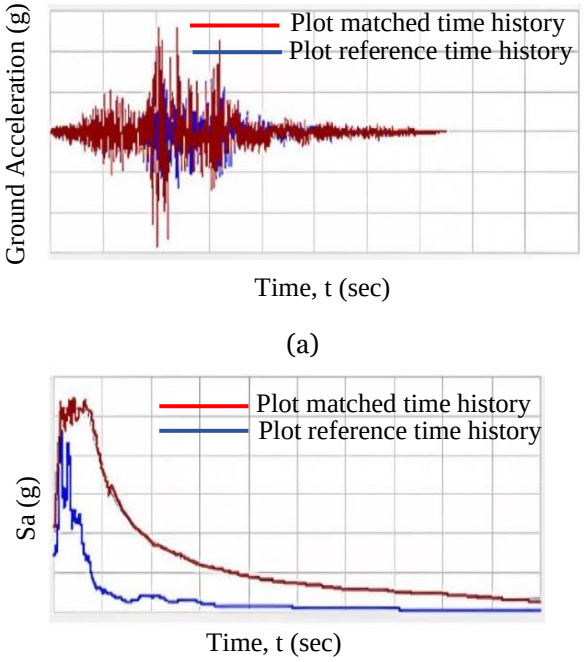

Figure 4: Isolations on the 1st (a) and Isolations on the 5th story (b)

3.4.2 Triple Friction Pendulum (TFP) Modeling

The triple friction pendulum isolations were placed at every column in a story or certain stories. The dimensions and properties of the TFP used are presented in Table 3:

Table 3: TFP dimension data

Properties	Value
$R_{1eff} = R_{4eff}$ (mm)	19585.21
$R_{2eff} = R_{3eff}$ (mm)	3030.06
$d_1^* = d_4^*$ (mm)	3118.857
$d_2^* = d_3^*$ (mm)	380.62188
$\mu_1 = \mu_4$ lower bound	0.10659
$\mu_2 = \mu_3$ lower bound	0.11625
μ lower bound	0.10801
$\mu_1 = \mu_4$ upper bound	0.12791
$\mu_2 = \mu_3$ upper bound	0.13951
μ upper bound	0.12970

3.4.3 Modeling of Isolated Building Structure

The model of Building Structure A with isolations on the 1 and 4th story is shown in Fig 5(a) and the model of Building Structure B with isolations on the 1 and 4th story is shown in Fig 5(b)

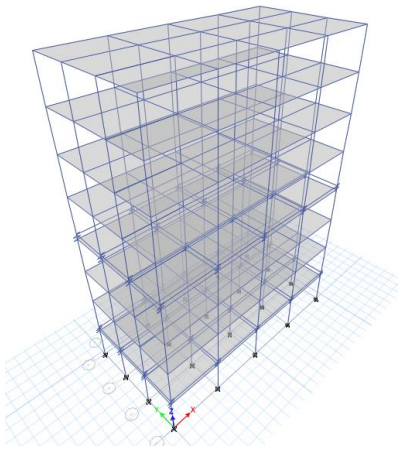

(a)

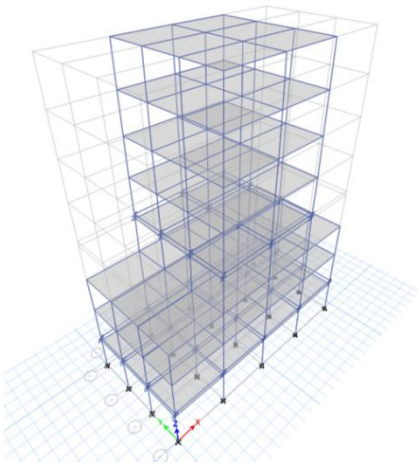

(b)

Figue 5: Deformed shape of Building Structure A (a) and B (b) model with isolations on the 1 and 4th story

3.4.4 Modeling of Isolated Building Structure

3.4.4.1 Building Period

Building Structure, A where the isolation location is on the 1st and 4th stories, has the largest period compared to other isolation placements, which is 2.499 seconds. The period of Building Structure A can be seen in Fig. 6(a), and Building Structure B, where the isolation location is on the 1st and 4th stories, has the largest period compared to other isolation placements, which is 2.042 seconds. The period of Building Structure B can be seen in Fig. 6(b).

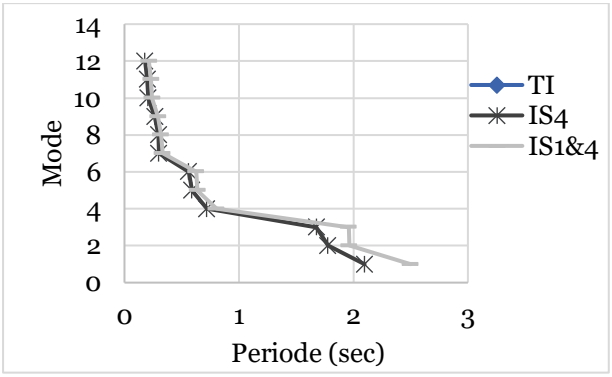

(a)

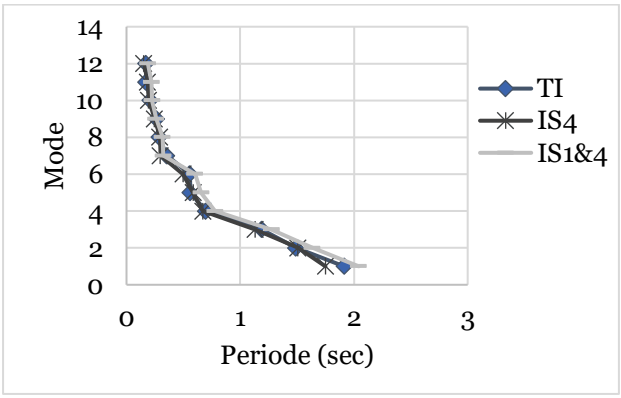

(b)

Figure 6: Period of Building Structure A (a) and Period of Building Structure B (b)

3.4.4.2 Inter-story Displacements

In SNI 1726:2019 Article 12.6.4.4 [19], Without isolator (TI) the largest x direction occurs in the imperial valley (IV) earthquake of 124,447 mm and the largest y direction occurs in the chi-chi (CT) earthquake of 163,689 mm. 4th-floor insulator (iso4) The largest x direction occurs in the super earthquake (SH) of 123,556 mm and the largest y direction occurs in the imperial valley (IV) earthquake of 157,247 mm. Insulator floors 1 and 4 (iso lt 1 & 4) The largest x direction occurs in the Imperial Valley (IV) earthquake of 126,832

mm and the largest y direction occurs in the chi-chi (CT) earthquake of 167,562 mm.

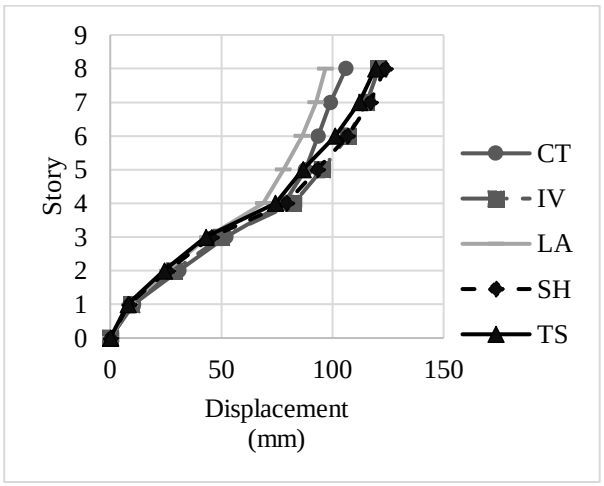

(a)

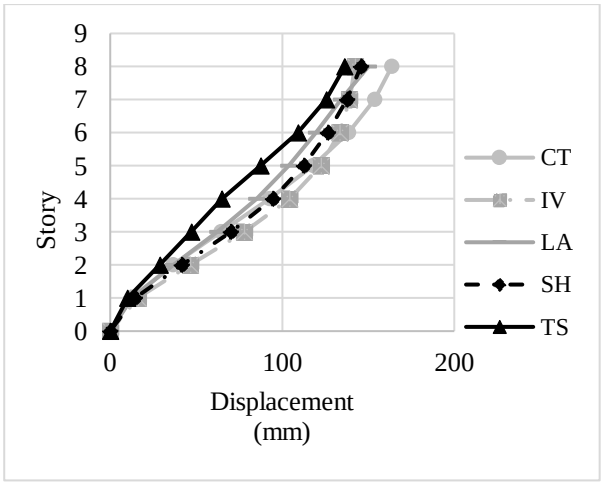

(b)

Figure 7: Inter-story displacements of Building Structure A x(a) and Inter-story displacements of Building Structure A y(b)

Comparative analysis Without isolators (TI) The largest x direction occurs in the chi-chi (CT) earthquake of 121,948 mm and the largest y direction occurs in the imperial valley (IV) earthquake of 160,967 mm. 4th-floor insulator (iso4) The largest x direction occurs in a chi-chi (CT) earthquake of 120,769 mm and the largest y direction occurs in a super earthquake (SH) of 150,287 mm. Insulator floors 1 and 4 (iso lt 1 & 4) The largest x direction occurred in the Taiwan earthquake (TS) of 125,325 mm and the largest y direction occurred in the Taiwan earthquake (TS) of 166,436 mm.

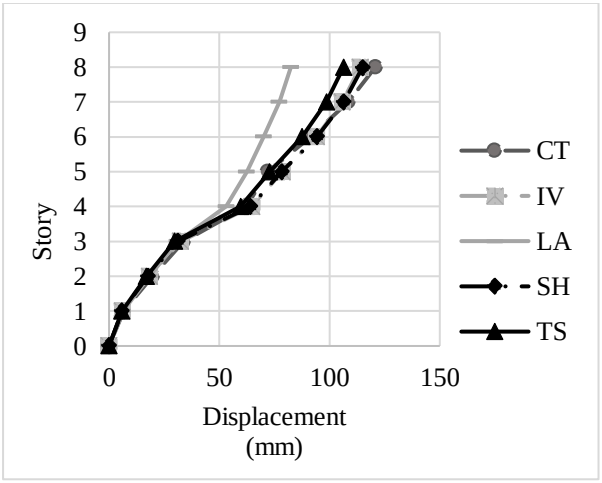

(a)

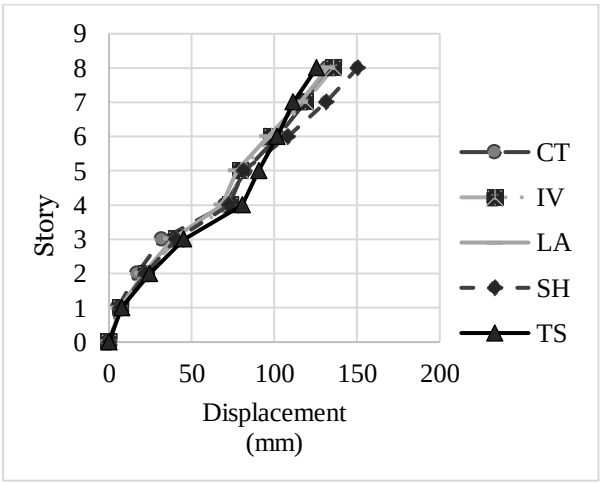

(b)

Figure 8: Inter-story displacements of Building Structure B x(a) and Inter-story displacements of Building Structure B y(b)

3.4.4.3 Internal Forces

The internal force on the largest column is at the insulator placement on floors 1 and 4 of 671.5127 kN, shear is 170.928 kN, and the moment is 431.8388 kN. The internal force on the largest beam is in the placement of the insulator on the 1st floor and 4th floor, shearing is 113,779 kN, and the moment is 238,985 kN.

Table 4: Internal forces column

Case	Aksial (kN)	Geser (kN)	Momen (kN.m)
IS4	636.0485	158.103	367.7744
IS1&4	671.5127	170.928	431.8388
TI	564.9624	155.8016	537.4191

Table 5: Internal forces beam

Case	Geser (kN)	Momen (kN.m)
IS4	105.715	200.268
IS1&4	113.779	238.985
TI	94.3351	210.1793

The internal force on the largest column is at the placement of the axial 1st and 4th-floor insulators of 613.2319 kN, shear of 148.6852 kN, and Moment of 343.9368 kN. The internal force on the largest beam is in the placement of the insulator on the 1st floor and 4th floor, shearing is 101.9542 kN, and the moment is 239.681 kN.

Table 6: Internal forces column

Case	Aksial (kN)	Geser (kN)	Momen (kN.m)
IS4	601.5762	176.2885	438.915
IS1&4	613.2319	148.6852	343.9368
TI	532.3182	154.4884	364.9997

Table 7: Internal forces beam

Base	Geser (kN)	Momen (kN.m)
IS4	100.76	222.787
IS1&4	101.9542	239.681
TI	89.876	219.874

3.4.4.4 Story Shear

Building level shear A is obtained from calculations with the help of a structural analysis program and is presented in the form of a graphical representation shown in Figure 8. Without isolators (TI) The largest x direction occurs in the landing earthquake (LA) of 2319.0267 mm and the largest y direction occurs in the imperial earthquake valley (IV) of 1908.557 mm. 4th-floor insulator (iso4) The largest x direction occurred in the Taiwan earthquake (TS) of 1811.9445 mm and the largest y direction occurred in the Taiwan earthquake (TS) of 4264.6802 mm. Insulators on the 1st and 4th floor (iso lt 1 & 4) the biggest x direction occurs in a chi-chi (CT) earthquake of 2592.4522 mm and the largest y direction occurs in a super earthquake (SH) of 2044.0243 mm.

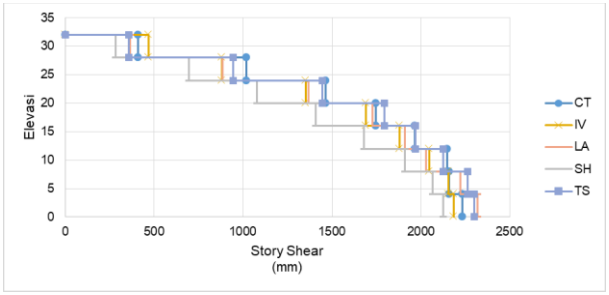

(a)

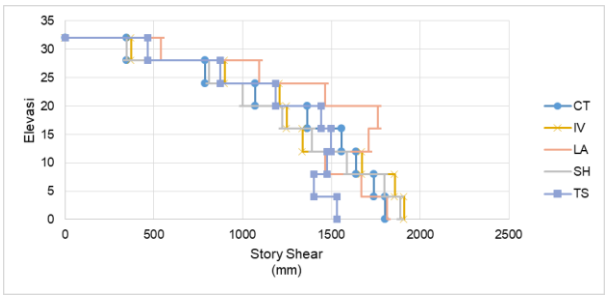

(b)

Fig 9. Story Shear of Building Structure A x(a) and Story Shear of Building Structure A y(b)

Building level shear B is obtained from calculations with the help of a structural analysis program and is presented in the form of a graphical representation shown in Figure 9. Without isolators (TI) The largest x direction occurs in earthquake landers (LA) of 1979.1134 mm and the largest y direction occurs in earthquake landers (LA) of 1983.4173 mm. Insulator 4th floor (iso4) The largest x direction occurs in a chi-chi (CT) earthquake of 1876.4601 mm and the largest y direction occurs in a super earthquake (SH) of 2235.5397 mm. Insulator floors 1 and 4 (iso lt 1 & 4) The largest x direction occurred in the Taiwan earthquake (TS) of 1909.5581 mm and the largest y direction occurred in the Taiwan earthquake (TS) of 1936.757 mm.

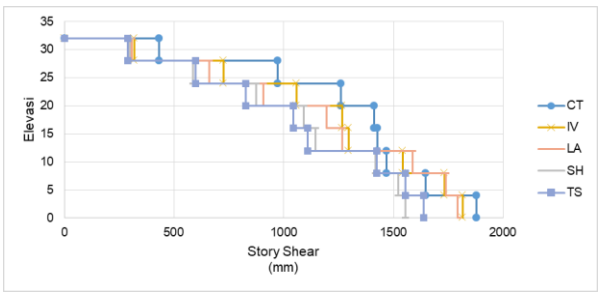

(a)

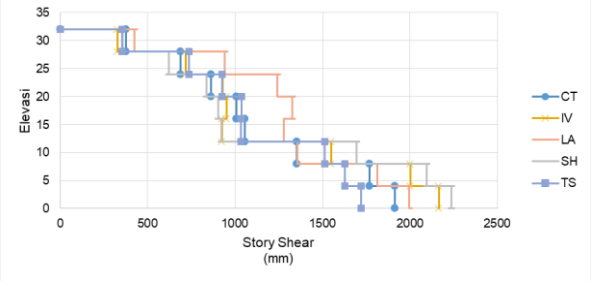

(b)

Fig 10. Story Shear of Building Structure B x(a) and Story Shear of Building Structure B y(b)

4. Discussion

The biggest structural response due to earthquake loads occurs when isolation is on floors 1 and 4, as seen from the results of the building period, the displacement between floors, floor shear, and internal forces. The placement of insulation with better results can be obtained when insulation is placed on two floors rather than on one floor and without insulation. The corresponding results obtained are more effective and better in minimizing structural damage. However, the placement of insulation is not suitable for insulation on the middle floor. The results show that the impact is not effective in terms of internal forces, story shear, and displacement between stories. Based on the analysis results obtained from the structural analysis program due to earthquake loads, it is known that the placement of insulation on the 1st and 4th floors gives the best response. Placing isolation on the 4th floor alone gives ineffective results due to earthquake loads both internal forces, shear between floors, and displacement between floors to minimize structural damage due to the impact of the earthquake. Meanwhile, the biggest earthquake that occurred was in the imperial valley based on the results of displacement, inter-story drift, and story shear.

5. Acknowledgments

The authors also gratefully acknowledge the financial support received from the Institut Teknologi Sepuluh Nopember for this work, under the project scheme of the Publication Writing and IPR Incentive Program (PPHKI) 2023.

References

[1] Wijaya, U., Soegiarso, R., Tavio., Wijaya, A., Numerical study of potential Indonesian rubber for elastomeric base isolators in highly-seismic zones, Journal of Physics: Conference Series, Vol. 1477, No. 5, 2020, pp. 1-7.

[2] Wijaya., U., Soegiarso, R., Tavio., Seismic performance evaluation of a base-isolated building, International Journal of Civil Engineering and Technology, Vol. 10, No. 1, 2019, pp. 285-296.

[3] Habieb, A.B., Milani, G., Tavio., Milani, F., Seismic performance of a masonry building isolated with low-cost rubber isolators, WIT Transactions on the Built Environment, Vol. 172, 2017, pp. 71-82.

[4] Habieb, A.B., Milani, G., Tavio., Milani, F., Low-cost frictional seismic base-isolation of residential new masonry buildings in developing countries: A small masonry house case study, Open Civil Engineering Journal, Vol. 11, No. M2, 2017, pp. 1026-1035.

[5] Tavio., Anggraini, R., Raka, IG.P., Agustiar., Tensile strength/yield strength (TS/YS) ratios of high-strength steel (HSS) reinforcing bars, AIP Conf. Proc., Vol. 1964, No. 020036, 2018, pp. 1-8.

[6] Wijaya, B.T.W., Tavio., Mechanical properties of Indonesian rubber for low-cost base isolation, International Journal of Civil Engineering and Technology, Vol. 10, No. 1, 2019, pp. 884-890.

[7] Harsono, B., Tavio., Tensile properties of fiberglass as reinforcement of low-cost rubber base isolator for small houses, International Journal of Civil Engineering and Technology, Vol. 10, No. 1, 2019, pp. 1933-1940.

[8] Rofiq, H.I., Tavio., Iranata, D., Model validation of carbon-fiber and glass-fiber reinforced elastomeric isolators using finite element method, IOP Conference Series: Earth and Environmental Science, Vol. 1116, No. 012001, 2022, pp. 1-12.

[9] Tavio., Purniawan, A., Behavior of rubber base isolator with various shape factors, AIP

Conference Proceedings, Vol. 1903, No. 020021, 2017, pp. 1-7.

[10] Zhou, F., Xiang, W., Zhu, H., Theoretical study of the double concave friction pendulum system under variable vertical loading, Advance in Structural Engineering, Vol. 22, No. 8, 2019, pp. 1-8.

[11] Tavio., Wijaya, U., Experimental study of Indonesian low-cost glass fiber reinforced elastomeric isolators (GFREI), International Journal on Advanced Science, Engineering and Information Technology, Vol. 10, No. 1, 2020, pp. 311-317.

[12] Ryan, K.L., Earl, C.L., Analysis and design of inter-story isolation system with nonlinear devices, Journal of Earthquake Engineering, Vol. 14, 2010, pp. 1044-1062.

[13] Almazan, J.L., de La Llera, J.C., Inaudi, J.A., Modelling aspects of structures isolated with the frictional pendulum system, Earthquake Engineering and Structural Dynamics, Vol. 27, No. 8, 2015, pp. 845-867.

[14] Wang, Y.P., Chung, L.L., Liao, W.H., Seismic response analysis of bridges isolated with friction pendulum behavior, Earthquake Engineering and Structural Dynamics, Vol. 27, No. 10, 2015, pp. 1069-1093.

[15] Shahabi, A.B., Ahari, Z. G., Barghian, M., Base isolation system-a state of the art review according to their mechanism, Journal of Rehabilitation in Civil Engineering, Vol. 8, No. 2, 2020, pp. 37-61.

[16] Fenz, D.M., Constantinou, M.C., Behaviour of the double concave friction pendulum bearing, Earthquake Engineering and Structural Dynamics, Vol. 35, No. 11, 2010, pp. 1403-1424.

[17] Fenz, D.M., Constantinou, M.C., Spherical sliding isolation bearings with adaptive behavior: experimental verification, Earthquake Engineering and Structural Dynamic, Vol. 32, No. 2, 2008, pp. 185-205.

[18] Schellenberg, A.H., Becker, T.C., Mahin, S.A., Hybrid shake table for the testing of midlevel seismic isolation system, 13th World Conference on Seismic Isolation, Paper No. 901421, 2013, pp. 1-9.

[19] National Standardization Agency. Procedures for planning earthquake resistance for building and non-building structures (SNI 1726:2019), BSN, Jakarta, 2019.

[20] National Standardization Agency. Structural concrete requirements for buildings (SNI 2847:2019), BSN, Jakarta, 2019.

[21] National Standardization Agency. Minimum design loads and related criteria for buildings and other structures (SNI 1727:2020), BSN, Jakarta, 2020.

[22] Fauzan., Ruddy, K., Nandaria S., Zev A. J., Dyan A. N. M., Curve Develops School Buildings With And Without Retrofit Due to Earthquake And Tsunami Loads, International Journal of GEOMATE, Vol. 24, No. 101, 2023, pp. 102-109.